

A Hybrid algorithm based on Bayesian Optimization and Interior Point OPTimizer for Optimal Operation of Energy Conversion Systems

Loukas Kyriakidis^a, Miguel Alfonso Mendez^b and Martin Bähr^a

^a German Aerospace Center, Cottbus, Germany, loukas.kyriakidis@dlr.de (CA), martin.baehr@dlr.de
^b von Karman Institute for Fluid Dynamics, Sint-Genesius-Rode, Belgium, miguel.alfonso.mendez@vki.ac.be

Abstract:

Optimization methods are essential to improve the operation of energy conversion systems including energy storage equipment and fluctuating renewable energy. Modern systems consist of many components, operating in a wide range of conditions and governed by nonlinear balance equations. Consequently, identifying their optimal operation (e.g. minimizing operational costs) requires solving challenging optimization problems, with the global optimum often hidden behind many local ones. In this work, we propose a hybrid method that advantageously combines Bayesian optimization (BO) and Interior Point OPTimizer (IPOPT). The BO is a global approach which exploits Gaussian process regression to build a surrogate model of the cost function to be optimized, while IPOPT is a local approach which uses quasi-Newton updates. The proposed BO-IPOPT combination allows leveraging the parameter space exploration of the BO with the quasi-Newton convergence of IPOPT once solution candidates are in the neighbourhood of an optimum. Using a challenging constrained test function, we test BO-IPOPT in accuracy, robustness and computational efficiency. Finally, we showcase the proposed hybrid method in the optimal operation of an industrial energy conversion system for renewable steam generation.

Keywords:

Nonlinear global optimization, Bayesian optimization, IPOPT, Hybrid method, Renewable steam generation.

1. Introduction

Numerical optimization is widely used to define the optimal operation [1–4] of energy conversion systems with many component combinations. A large number of system components, their interactions and included control parameters such as temperatures, mass flows or bypasses, combined with their nonlinear response, renders the optimization of these systems that are usually high dimensional and nonconvex. Yet, global optimization is required for model predictive control framework [5–7], where optimization methods with high accuracy and low computational cost are necessary.

Optimization methods can be classified into local and global, see e.g. [8,9]. Local methods use the information in the neighbourhood of a candidate solution to propose an update (improvement). Depending on whether the update relies on the cost function's gradient computation, these can be further classified as gradient-free (e.g. Nelder–Mead) and gradient-based (e.g. quasi-Newton methods). Local methods converge faster (i.e. with fewer cost function evaluations) than global ones if the starting point is sufficiently close to the optimum or if the cost function is (at least locally) convex. However, these methods are more prone to get stuck into local minima. A simple approach to mitigate this risk is to use multi-start (MS) algorithms [10], consisting in repeating the local optimization from multiple starting points. Leveraging the fast convergence of local methods, this approach can capture a large distribution of local optima, from which the one with the best objective function value can be taken as the best guess for the global optimum.

Global methods can be classified into deterministic and stochastic. Deterministic global optimization is mainly based on concepts of enumeration, generating cuts, and bounding to feasible regions that do not contain any optimal solution [9]. Nevertheless, commercial deterministic global solvers, like BARON [11], are extremely computational expensive especially in nonlinear nonconvex problems, where the CPU time increases exponentially with the number of variables and constraints. Common simplifications, which aim to reduce the complexity of the problem so that a global method like BARON can provide the global solution in reasonable time, are the linear modeling of system components [12] and the linearization of nonlinear component equations [13]. However, the former does not always guarantee a realistic system behaviour, whereas the latter requires an appropriate linearization technique depending on the model complexity, where a balance between accuracy and time efficiency must be found for the definition of the grid fineness.

An alternative to the deterministic global search is the random search of stochastic global optimization. These can be further classified into single candidate (e.g. simulated annealing) or population-based (e.g. genetic algorithms or particle swarms) [14] depending on the number of solutions that are iterated upon, or into metaheuristics or surrogate-based depending on the criteria used for the update. Metaheuristic methods (such as genetic algorithms or particle swarms) use a bio-inspired heuristic strategy to advance candidate solutions, while surrogate-based approaches (such as Bayesian optimization [15–18]) build a surrogate model of the function to optimize and use the model to drive the new evaluations. Global stochastic methods can avoid local minima, but tend to require a much larger number of cost-function evaluations than local ones.

The complementary advantages of these methods have motivated various hybrid approaches combining global and local methods [14, 19, 20]; the reader is referred to [21] for an overview of hybridization strategies. While most hybrid methods have combined metaheuristics with local methods, the recent focus seeks to combine surrogate-based methods and gradient-based optimization [22–24] to maximize the sample efficiency of the hybrid formulation.

This work explores the combination of Bayesian optimization and a quasi-Newton local approach to determine the optimal operation of energy conversion systems. In particular, we use the classic BO with Gaussian process regression (GPR) and expected improvement [15] together with the Interior Point OPTimizer (IPOPT) [25, 26]. Our combination is similar to the one proposed in [24], but differs in how the local method is integrated with the GPR, as further detailed in Section 2.3.

This paper is organized as follows: Section 2. gives an overview of the background of the proposed method BO-IPOPT. Section 3. presents the test cases analyzed in this work, namely a constrained test function with known global solution and the constrained optimization problem arising from the operational management of a renewable steam generation system to test the performance of our proposed method. Finally, Section 4. summarizes the main conclusions and provides perspective for future works.

2. Optimization Methods

In this work, we consider the general constrained optimization problem, defined as:

$$\min_{\mathbf{x} \in \Omega} \left\{ f(\mathbf{x}) \text{ s. t. } \mathbf{h}(\mathbf{x}) = \mathbf{0}, \mathbf{g}(\mathbf{x}) \leq \mathbf{0} \right\} \quad (1)$$

with $\mathbf{x} \in \Omega \subseteq \mathbb{R}^n$ the n -dimensional decision variable contained in set Ω , $f : \mathbb{R}^n \rightarrow \mathbb{R}$ the objective function, $\mathbf{h} : \mathbb{R}^n \rightarrow \mathbb{R}^p$ the set of equality constraints, and $\mathbf{g} : \mathbb{R}^n \rightarrow \mathbb{R}^q$ the set of inequality constraints. The functions $f, \mathbf{h}, \mathbf{g}$ can be nonlinear and nonconvex, but are assumed to be sufficiently smooth.

We aim to develop an optimization method that provides a sequence of candidate solutions $\{\mathbf{x}_K\}$ converging towards the global minimum $\mathbf{x}_K \rightarrow \mathbf{x}^*$ with the highest probability and the fewer iterations K . In what follows, we briefly introduce the BO and IPOPT methods and motivate our interest in their combination.

2.1. Bayesian Optimization (BO)

BO is a global black-box optimization approach, i.e. requiring no mathematical definition of the objective function. The main idea is to use the sampling at the candidate solutions $\{\mathbf{x}_K\}$ to build a surrogate model of the cost function. Following [15], the surrogate model is usually built with GPR, which is a kernel regression method [27] allowing the analytical computation of both the regression and its uncertainties. The uncertainties of the model can be used to balance exploitation, i.e. the tendency to sample where the surrogate predicts best objective values, with exploration, i.e. the tendency to sample where the surrogate has the highest uncertainty. An approach to deal with optimization constraints is to augment the objective function as follows according to [14]:

$$u(\mathbf{x}) = f(\mathbf{x}) + \rho \mathbf{h}(\mathbf{x})^2 + \lambda \max(\mathbf{0}, \mathbf{g}(\mathbf{x}))^2 \quad (2)$$

where $\rho, \lambda \geq \mathbf{0}$ are penalty weight vectors associated with the magnitude of constraint violation. The two ingredients in the BO are described as follows:

1. *GPR*: The GPR builds the surrogate model considering it as a Gaussian process (GP), i.e. a multivariate Gaussian distribution in the domain Ω . This distribution is initialized with a *prior* mean $m(\mathbf{x})$ and covariance defined by a kernel function, usually taken as a Gaussian $k(\mathbf{x}, \mathbf{x}') = \exp(-d(\mathbf{x}, \mathbf{x}')^2/2l^2)$, with l the length scale of the kernel and $d(\cdot, \cdot)$ the Euclidean distance between points in Ω . As sample points $\{\tilde{\mathbf{x}}_1, \dots, \tilde{\mathbf{x}}_{N_c}\}$ and associated objective values $\tilde{u}_n = u(\tilde{\mathbf{x}}_n)$ are collected, the GPR updates the underlying GP using standard conditioning rules [27] such that the (surrogate) predictions in $\mathbf{x} \in \Omega$ become $\hat{u}(\mathbf{x}) \sim \text{GP}(\mu(\mathbf{x}), \Sigma(\mathbf{x}))$ with mean $\mu(\mathbf{x})$ and covariance $\Sigma(\mathbf{x})$ functions defined as:

$$\mu(\mathbf{x}) = \mathbf{K}_*^T (\mathbf{K}_{**} + \alpha \mathbf{I})^{-1} u(\tilde{\mathbf{x}}) \quad \text{and} \quad \Sigma(\mathbf{x}) = \mathbf{K} - \mathbf{K}_*^T (\mathbf{K}_{**} + \alpha \mathbf{I})^{-1} \mathbf{K}_* \quad (3)$$

where $\mathbf{K} = k(\mathbf{x}, \mathbf{x})$, $\mathbf{K}_* = k(\mathbf{x}, \bar{\mathbf{x}})$, $\mathbf{K}_{**} = k(\bar{\mathbf{x}}, \bar{\mathbf{x}})$, \mathbf{I} is the identity matrix of appropriate size and α is a regularization parameter that avoids the fully interpolative behaviour of the GPR. The main hyperparameters of the regression are the kernel's length scale l and the regularization α ; the first determines the smoothness of the function, while the second regularizes the sensitivity of the regression towards noise in the case of stochastic objective functions.

2. *Acquisition function*: This function controls the location of the new candidate solutions. The common approach, also used in this work, is to use the expected improvement (EI) function. This is defined as:

$$\text{EI}(\mathbf{x}) = \begin{cases} (\hat{u}(\mathbf{x}^*) - \mu(\mathbf{x}) - \xi)\Phi(Z) + \sigma(\mathbf{x})\phi(Z) & \text{if } \sigma(\mathbf{x}) > 0 \\ 0 & \text{if } \sigma(\mathbf{x}) = 0 \end{cases} \quad \text{with } Z = \begin{cases} \frac{\hat{u}(\mathbf{x}^*) - \mu(\mathbf{x}) - \xi}{\sigma(\mathbf{x})} & \text{if } \sigma(\mathbf{x}) > 0 \\ 0 & \text{if } \sigma(\mathbf{x}) = 0 \end{cases} \quad (4)$$

where Φ and ϕ denote the cumulative distribution function and the probability distribution function, respectively. The first term controls the exploitation: this term is large if the new samples are close to the expected optima according to the surrogate model. The second term controls exploration: this term is large if the new samples are in the area of large $\sigma(\mathbf{x}) = \text{diag}(\boldsymbol{\Sigma})$. The parameter ξ sets a threshold over the minimal expected improvement that justifies the exploration and is a hyperparameter of the BO; hence the larger this value, the more exploration is produced.

In the classic BO, the algorithm begins with a set of randomly chosen candidate solutions and iterates alternating one update of the GPR and the maximization of EI to define new candidates.

2.2. Interior Point OPTimizer (IPOPT)

The open-source software package IPOPT [25] is a popular tool for solving large-scale nonlinear optimization problems. The solver is mainly based on a primal-dual interior-point method combined with a filter line-search method [26]. IPOPT can also be applied to nonconvex problems, but should be at least once, ideally twice, continuously differentiable.

Algorithmically, IPOPT transforms any inequality constraints of the original problem (1) into natural logarithmic barrier terms in the objective function, including a barrier parameter, thus considering a parametric problem. Based on this, a sequence of equality-constrained problems (barrier problems) is solved for decreasing values of the mentioned barrier parameter. This approach is repeated until a point satisfies the first-order Karush-Kuhn-Tucker optimality conditions. Note that also maximizers and saddle points satisfy the latter optimality conditions, but IPOPT internally uses a Hessian regularization that avoids obtaining maximizers and saddle points. For each barrier sub-problem, a Newton-type algorithm with line search is applied, including the solution of indefinite sparse symmetric linear systems. In particular, the overall performance (runtime, accuracy and robustness) strongly depends on the properties of the chosen sparse linear solver.

Overall, IPOPT is a highly efficient solver to find a local solution of a large-scale nonlinear nonconvex constrained optimization problem. However, the computed local optimum depends strongly on the selected starting point. Consequently, the initialization determines the rate of convergence to a solution and to which optimum the algorithm converges. It should be noted that the local optimization method can also perform poorly and even fail if the initial guess is unfavorable.

2.3. Hybrid Method BO-IPOPT

The proposed BO-IPOPT combination is illustrated in Algorithm 1. The algorithm starts with a set of initialization points to generate a first surrogate model via GPR (cf. lines 1-4). In doing so, the evaluation of the initialization points is possible, since the objective function is assumed to be known. The main part of the algorithm consists of alternating steps of BO and IPOPT until the total number of outer iterations K is satisfied (cf. lines 6-13). More specifically, new candidates for the GPR are first selected by evaluating the acquisition function EI. However, instead of updating the surrogate model directly with the newly selected candidates (as in classical BO), IPOPT is applied to the best candidates, so the surrogate model is then updated based on these local optima. It should be noted that the proposed approach uses only feasible solutions (in line 9): if the solution of IPOPT is not feasible, the algorithm selects the next best candidate.

The advantage of the proposed BO-IPOPT method is that IPOPT increases the convergence of the BO by moving some of the candidate solutions towards optimal locations. When these are local optima, the EI evaluation allows for maintaining global exploration and improving the regression where needed. If any of these is a global optimum, the EI keeps favouring its sampling in the following iterations. Overall, this method is not only efficient for BO to speed up its convergence but also for IPOPT to effectively determine good initial points. It is worth noticing that any local solver could replace IPOPT, which was chosen here because of its efficient, robust, open-source implementation.

As mentioned in Section 1., the recently proposed approach BOWLS [24] (cf. corresponding Algorithm 3 in the mentioned article) is similar to ours. In [24], the BO framework is also used to determine the local solver's

Algorithm 1 Hybrid Method BO-IPOPT

Input: length scale l ; regularization term α of GPR; amount of exploration ξ ; number of initialization points N_0 ; number of candidates N_c considering in EI; number of best candidates N_{bc} selected at each iteration; penalty weight vectors ρ, λ ; number of outer iterations K ;

- 1: generate a number of points $\{\mathbf{x}_1, \dots, \mathbf{x}_{N_0}\}$ in Ω ;
- 2: evaluate $y_n = u(\mathbf{x}_n)$ for $n = 1 : N_0$;
- 3: let $D_0 = \{(\mathbf{x}_n, y_n)\}_{n=1}^{N_0}$;
- 4: construct a GPR model \hat{u}_0 from D_0 ;
- 5: $n = N_0, j = 0$;
- 6: **while** $j < K$ **do**
- 7: generate a new group of points $\{\bar{\mathbf{x}}_1, \dots, \bar{\mathbf{x}}_{N_c}\}$ in Ω ;
- 8: $\{\mathbf{x}_{n+1}, \dots, \mathbf{x}_{n+N_{bc}}\} = \arg \max \text{EI}(\bar{\mathbf{x}}_i; \hat{u}_n)$ for $i = 1 : N_c$;
- 9: solve $[y_k^*, \mathbf{x}_k^*] = \text{IPOPT}(\mathbf{x}_k)$ for $k = n + 1 : n + N_{bc}$;
- 10: $D_{j+1} = D_j \cup \{(\mathbf{x}_{n+1}^*, y_{n+1}^*), \dots, (\mathbf{x}_{n+N_{bc}}^*, y_{n+N_{bc}}^*)\}$;
- 11: update GPR model \hat{u}_{j+1} from D_{j+1} ;
- 12: $n = n + N_{bc}, j = j + 1$;
- 13: **end while**
- 14: **return** $y_{\min} = \min\{y_i\}_{i=1}^n$;

Algorithm 2 MS-IPOPT

Input: Number of outer iterations K ;

- 1: **for** $i = 1 : K$ **do**
- 2: generate a random point \mathbf{x}_i in Ω ;
- 3: solve $[y_i^*, \mathbf{x}_i^*] = \text{IPOPT}(\mathbf{x}_i)$;
- 4: **end for**
- 5: **return** $y_{\min} = \min\{y_i^*\}_{i=1}^K$;

starting points and thus create a suitable MS formulation. However, it should be noted that there are some technical differences to our version. First, the initial GPR model is built from the results of the local searches (not random ones); this brings the risk of restricting the sampling region of the GPR. Second, the initial and updated GPR models are based on the value of the objective function from the local optima but on the inputs of the initial points *before* using the local solver (\mathbf{x} instead of \mathbf{x}^*). Consequently, the GPR at each iteration does not approximate the underlying function but another one that shares the same local minima identified thus far. Finally, BOwLS uses the conjugate gradient method from the SciPy package as a local search, thus not accounting for constraints and the feasibility set of the problem.

3. Numerical Examples

In this section, we showcase the proposed BO-IPOPT approach on (i) a test function and (ii) the optimization of a renewable steam generation system. In both test cases, the performance of BO-IPOPT is compared with the classical random-based MS-IPOPT (cf. Algorithm 2) and the BOwLS [24] in terms of accuracy, CPU time and robustness. All algorithms were implemented in Python 3.8. More specifically, BO was implemented using the sklearn library [28] for the GPR, while IPOPT is used via the Python Optimization Modeling Objects (Pyomo) software package [29]. To provide the first and second derivative, Pyomo uses the automatic differentiation features in the Ampl Solver Library.

All computations were carried out on a machine with Intel(R) Core(TM) i7-8665U CPU. To allow for a fair comparison between hybrid approaches, we implement IPOPT as the local solver for the BOwLS since the conjugate gradient method from the SciPy package used in [24] is not designed to handle constrained problems. Additionally, for consistency, we consider the same parameters for both hybrid methods, i.e. $N_0 = 10$, $N_c = 1,000$, $N_{bc} = 2$, $\xi = 0.01$, $\alpha = 0.1$, $l = \rho = \lambda = 100$, and the same acquisition function EI. Concerning the random-based MS-IPOPT, we implement it with $N_{bc} = 2$ (cf. line 2 in Algorithm 2), meaning that two random points are generated for each outer iteration K and used as starting points for the IPOPT solver.

3.1. Constrained Ackley Function

The first test case is the well-known Ackley function, often used to test optimization algorithms [30]. This function is nonconvex and highly multi-modal with multiple local minima and one global minimum. Since the Ackley function was originally designed as an unconstrained optimization test case, we add two inequality

constraints as in [30]. The resulting constrained optimization problem is defined as follows:

$$\min -20 \exp \left(-0.2 \sqrt{\frac{1}{n} \sum_{i=1}^n x_i^2} \right) - \exp \left(\frac{1}{n} \sum_{i=1}^n \cos(2\pi x_i) \right) + 20 + e \quad (5)$$

$$\text{s. t. } \sum_{i=1}^n x_i \leq 0, \quad \|\mathbf{x}\|_2 - 5 \leq 0, \quad \mathbf{x} \in [-5, 10]^n \quad (6)$$

where n denotes the problem's dimension, set to $n = 100$ for this experimental study. The optimization problem (5)-(6) has a global minimum at $\mathbf{x} = \mathbf{0}$ with objective function value 0, i.e. $f(\mathbf{x}) = 0$. Since all implemented algorithms are based on a certain randomness, our numerical experiments were repeated 100 times with a number of outer iterations $K = 300$.

The optimization results of all three methods are shown in Fig. 1. The figure on the left compares the averaged minimum objective function value, while the figure on the right compares the averaged CPU time versus the number of outer iterations. It can be seen that the proposed BO-IPOPT outperforms the others in convergence and robustness. As expected, MS-IPOPT and BO-IPOPT start with a higher minimum objective function value than BOwLS because both methods use a random initialization, while BOwLS considers local optima as initialization for the initial GPR model. Obviously, BO-IPOPT converges faster towards the global minimum, which can be explained as follows: on the one hand, MS-IPOPT naturally converges more slowly to the global optimum because it strongly depends on its randomly chosen starting points. On the other hand, the GPR in BO-IPOPT has better performance in providing a better surrogate model since the sampling is more spread than in BOwLS, which narrows the sampling near the local optima. Regarding CPU time, the simplest MS-IPOPT outperforms both hybrid methods, as shown on the right side of Fig. 1; this gives an order of magnitude of the costs for training the GPR surrogate model in the two hybrid methods.

It should be underlined that an exhaustive comparison of the two hybrid methods should also include a broader range of hyperparameters; this will be carried out in the extended version of this work. For the investigated test case, the performance gap appears to depend on the outer iterations K : as shown in Fig.1, at $K = 100$, BO-IPOPT is well ahead in the averaged minimum objective function value, but BOwLS reaches similar objectives at $K \approx 170$. The number of initialization points N_0 is a second crucial parameter. It is expected that larger values will favour BO-IPOPT, since they enable better exploration of the solution space, while the local optimization in BOwLS restricts the exploration of the BO. Moreover, increasing N_0 increases the number of (initial) local searches in the BOwLS and thus directly leads to higher computational costs, in contrast to BO-IPOPT. Finally, the number of local searches before the updating of the GPR model is expected to have a significant impact on the balance between accuracy and computational cost and will also be investigated in future work.

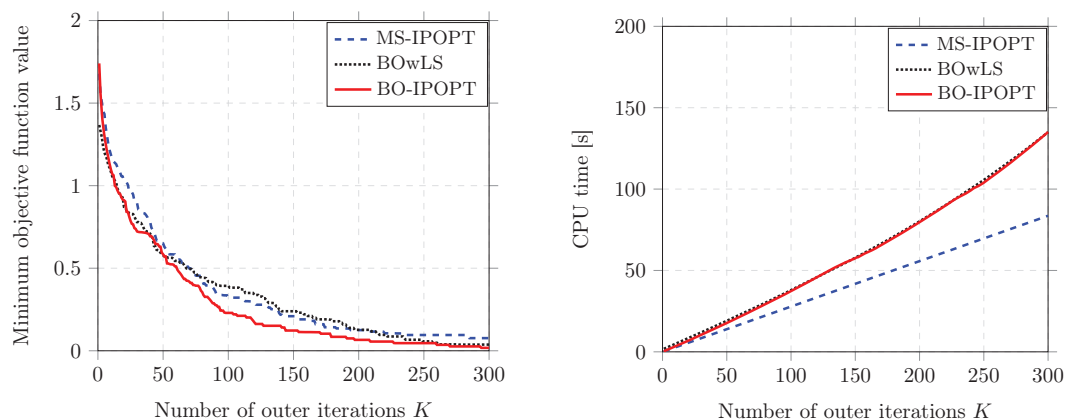


Figure 1: Optimization results for the constrained Ackley function (5)-(6): comparison of the averaged minimum objective function value (**left**) and averaged CPU time (**right**) over 100 trials using MS-IPOPT, BOwLS and BO-IPOPT in relation to the number of outer iterations K .

3.2. Renewable Steam Generation

The second test case is the operation optimization problem of an industrial energy conversion system for renewable steam generation. This power-to-heat system (cf. Fig. 2) was recently proposed in [31] and is currently used as a practical benchmark to evaluate the algorithms. In the following, we first briefly describe the test case and the resulting optimization problem (Section 3.2.1.) and then present and discuss the results of the optimization (Section 3.2.2.).

3.2.1. Problem Description

The considered electrified system shown in Fig. 2 aims to provide constant process heat in the form of superheated steam for an industrial process. The multi-component system mainly consists of 4 units: (i) a wind turbine (WT) to produce renewable electricity driving the system; (ii) a closed reverse Brayton cycle high-temperature heat pump (HTHP), powered by electricity from the WT or the power grid, to generate process heat; (iii) a sensible thermal energy storage (TES) to store excess thermal energy generated during periods of high wind power or low electricity prices; (iv) the steam generator (SG) for providing process steam via an intermediate thermal oil stream and controllable fluid bypasses.

The HTHP and SG models were created with a process simulation software, with the former being able to simulate part load behaviour. The TES model is developed using a lumped capacitance approach, while the WT power output is modeled from the specific power curve at hub height, i.e. the power curve determines the wind power generated as a function of the wind speed extrapolated to the corresponding height.

In the system configuration (cf. Fig. 3), the HTHP provides high-temperature process heat to an intermediate circuit routed through the TES or directly to the SG via a controllable fluid bypass. Thermal oil is chosen as heat transfer fluid (HTF) in the intermediate loop due to its compactness and fluid phase within the temperature range. During the charging process, the temperature in the TES is heated up by the HTF before it enters the SG; discharging operation is vice versa. In discharge mode, the HTHP's power consumption can be significantly reduced since less heat has to be supplied to the intermediate loop to ensure constant steam generation. In idle operation, the TES is completely bypassed by the HTF. The cold outlet stream is not used for cooling applications in the current setup. For more details, we refer the reader to [31].

Optimization aims to determine the cost-optimal operation, i.e. minimizing operational costs considering the fluctuating wind energy and electricity prices. To build an algebraic model problem, the underlying HTHP and SG models are converted into an algebraic form using polynomial surrogate models, as described in [31]. This results in an algebraic nonlinear nonconvex constrained optimization problem that can be formulated in a discrete setting as:

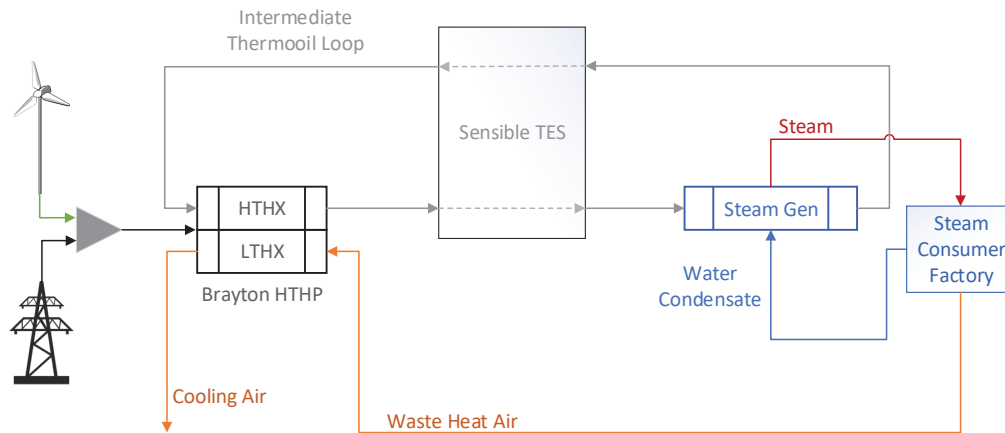


Figure 2: Illustration of the investigated industrial energy conversion system for electrified steam generation recently proposed in [31]. The system consists of a HTHP, a TES and a SG, where the HTHP is powered by electricity from a wind turbine or the power grid. The HTHP uses waste heat air stream as a heat source and enables charging and discharging of the TES via an intermediate thermal oil stream. Furthermore, constant heat demand for the steam consumer factory must be satisfied.

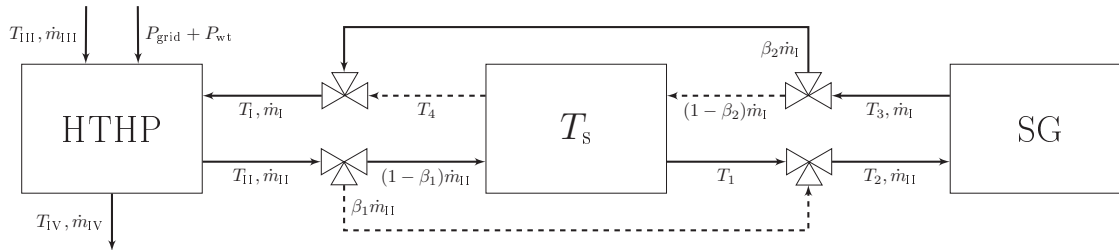


Figure 3: Detailed flow chart [31] of studied system (cf. Fig. 2) including HTHP, TES and SG. HTHP and SG are represented by polynomial surrogate models, while TES is modeled by an effectiveness model. An adjustable fluid bypass $\beta_1 \in [0, 1]$ is used to control the heat input to the TES and SG, conversely the bypass $\beta_2 \in [0, 1]$ regulates the heat input to the HTHP depending on the thermal state T_s of the TES and SG outlet stream. The *solid* and *dashed* lines indicate the charging and discharging mode in a simplified way. In addition, simultaneous charging and discharging is not allowed. For example, *charge* mode is $\beta_1 \in [0, 1], \beta_2 = 1$, *discharge* mode implies $\beta_2 \in [0, 1), \beta_1 = 1$, and *idle* mode represents $\beta_1 = \beta_2 = 1$.

$$\min J(P_{\text{grid}}) = \sum_{k=1}^n P_{\text{grid}}^k \Delta t \quad (7)$$

s. t.

$$P_{\text{grid}}^k + P_{\text{wt}}^k = 3F_{\text{HTHP}}(T_{\text{II}}^k, \dot{m}_I^k, T_{\text{III}}^k, R^k), \quad T_{\text{II}}^k = F_{\text{HTHX}}(T_1^k, \dot{m}_I^k, T_{\text{III}}^k, R^k), \quad T_{\text{IV}}^k = F_{\text{LTHX}}(T_1^k, \dot{m}_I^k, T_{\text{III}}^k, R^k) \quad (8)$$

$$T_2^k = T_{\text{II}}^k \beta_1^k + T_1^k (1 - \beta_1^k), \quad T_1^k = T_3^k \beta_2^k + T_4^k (1 - \beta_2^k) \quad (9)$$

$$T_2^k = 201.92 + \frac{1819.32}{3\dot{m}_I^k}, \quad T_3^k = 196.3 - \frac{188.4}{3\dot{m}_I^k} \quad (10)$$

$$\dot{Q}_{\text{s, ch}}^k = 3\dot{m}_{\text{II}}^k c_{p, f}(T_{\text{II}}^k - T_1^k)(1 - \beta_1^k), \quad \dot{Q}_{\text{s, dch}}^k = 3\dot{m}_I^k c_{p, t}(T_4^k - T_3^k)(1 - \beta_2^k), \quad \dot{Q}_{\text{s, ch}}^k - \dot{Q}_{\text{s, dch}}^k \leq \gamma \quad (11)$$

$$T_1^k = T_{\text{II}}^k - \epsilon_{\text{ch}}(T_{\text{II}}^k - T_s^{k-1}), \quad T_4^k = T_3^k - \epsilon_{\text{dch}}(T_3^k - T_s^{k-1}), \quad T_s^k = T_s^{k-1} + \frac{\dot{Q}_{\text{s, ch}}^k - \dot{Q}_{\text{s, dch}}^k}{m_s c_{p, s}} \Delta t \quad (12)$$

$$T_s^0 = \tilde{T}_0, \quad T_s^n = T_s^0 \quad (13)$$

$$T_{\text{II}}^k \in [177, 250], \quad \dot{m}_I^k \in [5, 16], \quad T_{\text{III}}^k \in [60, 100], \quad R^k \in [0.8, 1.53] \quad (14)$$

with a uniformly spaced time grid $t_k = \Delta t_k$ for $k = 1, \dots, n$, so that the functions are considered only at the discrete time points, i.e. $T_I^k := T_I(t_k)$. The linear objective function (7) relies on the system's operating cost that is directly related to the consumed grid power of the HTHP. The power balance and outlet temperatures of the HTHP are described by (8), where F_{HTHP} , F_{HTHX} , and F_{LTHX} represent the corresponding surrogate models as a function of inlet temperatures, mass flow and rotational shaft speed. The bypass modeling is represented by (9), while (10) reflects the SG surrogate models. The charging and discharging heat flows (11) depend on the HTF mass flow, the temperature level and the fluid flow bypasses. Moreover, charging and discharging at the same time is not allowed. The constraints (12) relate to the TES effectiveness model and the storage temperature change. For a complete set-up, an initial storage temperature \tilde{T}_0 is required, which is assumed to be the same at the end of the operating period (13). The simplified models in (8) are valid within the box constraints in (14), while other variables are naturally limited by the system itself. The factor 3 in (8), (10) and (11) arises because the surrogate models were derived for a single HTHP, but three HTHPs are operated in parallel to keep the component dimensions within a moderate scale.

3.2.2. Optimization Results

This section presents the optimization results of the proposed system for renewable steam generation. We consider a one-day system operation and set the time step to $\Delta t = 1$ h, giving the total number of discrete steps $n = 24$. The scenario for the WT power production and the grid electricity price are displayed in Fig. 4

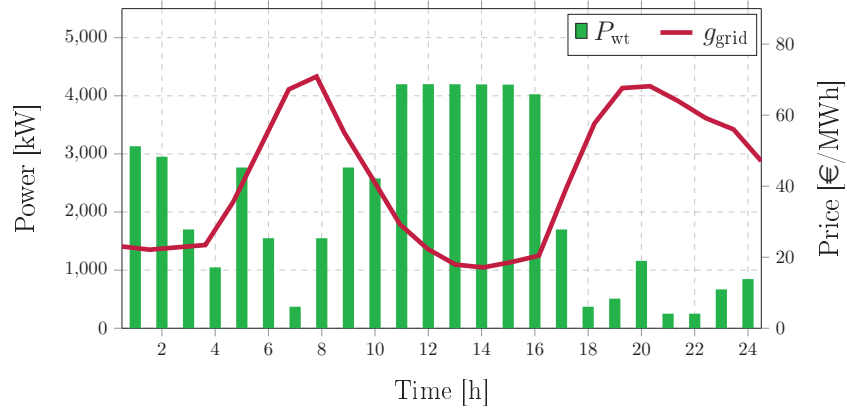


Figure 4: Visualization of 24h reference data P_{wt} (WT power output) and $g_{pr,grid}$ (electricity price) to minimize operating cost in (7)-(14).

as a function of time during 24h. The time horizon considered, resulting in 408 decision variables controlling the system, makes this test case unfeasible for a commercial global optimization solver like BARON.

The optimization results are presented in Fig. 5. As in Section 3.1., we compare the performance of the proposed BO-IPOPT to MS-IPOPT and BOWLS. The same hyperparameters as in the previous test case are considered. Our numerical experiments are repeated 20 times for averaging out the stochastic nature of the optimizers. We reduce this number with respect to the previous test case because this optimization problem requires larger computational time due to the larger dimension and the large set of equality constraints. Since the global minimum of this optimization problem is unknown, we use MS-IPOPT with 10,000 different initialization points to explore the parameter space. The best result, herein considered as an estimate of the global optimum, lies at 1,046.53€. This optimum is shown in Fig. 5 on the left.

As in the previous test case, BO-IPOPT outperforms the other approaches in convergence and robustness, while both hybrid methods converge faster towards the best reference solution than the MS-IPOPT. The same observations made from the previous test case on the role of the initial point for BO-IPOPT and BOWLS apply to this case. However, it is worth noticing that none of the optimizers approach the best known solution (estimated by the 10,000 IPOPT iterations) within the $K = 300$ outer iterations on average. This, together with the minor improvements achieved by all optimizers, highlights the complexity of the optimization problem at hand. In terms of computational cost, Fig. 5 on the right shows a nearly linear trend for both the hybrid methods and the MS-IPOPT, with the slope being much larger than in the previous test case because of the larger dimensionality of the problem. Nevertheless, this shows that the increased computational cost of the GPR, produced as more samples are available, weighs much less than the objective function evaluation itself for the number of initialization points ($N_0 = 10$) considered in this test case.

The choice of hyperparameters clearly influences the performance of both hybrid methods. Among these, the number of candidates N_{bc} updated via the local solver appears a critical parameter governing the optimization convergence as well as the computational effort. Fig. 6 shows the impact of this hyperparameter in the optimization convergence, both in terms of average convergence and CPU time. A significant increase in the computational cost results in a minor improvement in the convergence. This highlights that much of the cost in the hybrid formulation is due to the local solver and not the GPR updating. Future work will analyze the impact of various hyperparameters in optimization performance with the proposed hybrid method in more depth.

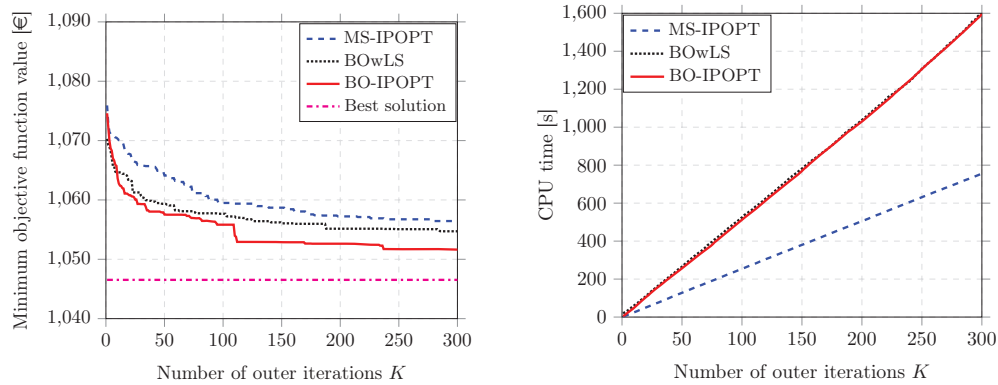


Figure 5: Optimization results for the use case renewable steam generation (7)-(14): comparison of the averaged minimum objective function value (**left**) and averaged CPU time (**right**) over 20 trials using MS-IPOPT, BOwLS and BO-IPOPT in relation to the number of outer iterations K . The best known solution (computed by 10,000 IPOPT iterations) is also visualized as an estimate of the global optimum on the left in the figure.

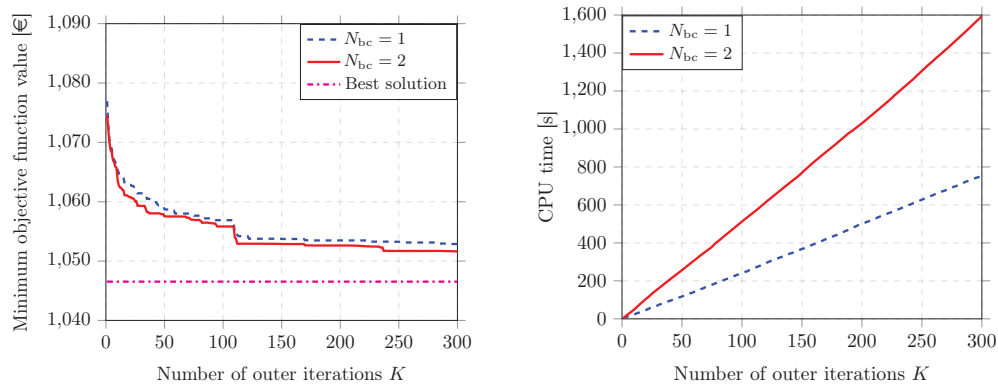


Figure 6: Optimization results for the use case renewable steam generation (7)-(14): comparison of the averaged minimum objective function value (**left**) and averaged CPU time (**right**) over 20 trials using BO-IPOPT with $N_{bc} = 1$ and $N_{bc} = 2$ in relation to the number of outer iterations K . The best known solution (computed by 10,000 IPOPT iterations) is also visualized as an estimate of the global optimum on the left in the figure.

4. Conclusion

This work presents a novel method called BO-IPOPT to determine the optimal operation of energy conversion systems. BO-IPOPT beneficially combines Bayesian optimization and Interior Point OPTimizer, allowing profit from the global exploration of the surrogate modelling in the BO with the quasi-Newton local convergence. In BO-IPOPT, BO is made aware of the constraints via penalty terms in the objective function, while IPOPT is naturally aware of the constraints during its updates.

We demonstrate the proposed method in a challenging constrained test case and the optimization of a complex industrial energy conversion system for renewable steam generation. The optimization performance is compared to the classical MS-IPOPT with random initialization and the recently introduced hybrid BOwLS. In both cases, the proposed hybrid method outperforms BOwLS and MS-IPOPT in convergence rate and robustness. The performance gain with respect to BOwLS appears to be linked to the different initialization criteria and the use of surrogate models that approximate the original function. Regarding the computational cost, the overhead of the hybrid methods is mostly linked to the construction of the GPR at each iteration. Nevertheless, this is found to be negligible in both cases. On the other hand, the major increase in the CPU time for both hybrid methods is primarily due to the additional number of best candidates leading directly to more IPOPT evaluations. However, these can be carried out independently and could be easily parallelized. This will be the subject of future work. Finally, future work will address the problem of hyperparameter optimization for BO-IPOPT and consider the sensitivity of its performance to identify the optimal balance between accuracy and computational cost.

Acknowledgments

The authors declare no competing interests. This research did not receive any specific grant from funding agencies in the public, commercial, or not-for-profit sectors.

Nomenclature

Letter symbols

| | |
|-------------------|---------------------------------------|
| c | specific heat capacity, J/(kgK) |
| D | set of points |
| $d(\cdot, \cdot)$ | Euclidean distance |
| El | expected improvement |
| F | surrogate model |
| f | objective function |
| g | set of inequality constraints |
| g | electricity price, €/MWh |
| h | set of equality constraints |
| I | identity matrix |
| J | operating costs, € |
| K | kernel matrix |
| K | number of outer iterations |
| k | kernel function |
| l | length scale |
| \dot{m} | mass flow, kg/s |
| m | mass, kg |
| N | number of points |
| n | number of dimensions |
| P | electric power, kW |
| \dot{Q} | heat flow rate, kW |
| R | rotational shaft speed |
| T | temperature, °C |
| \bar{u} | objective value of u at \bar{x} |
| \hat{u} | GPR model of u |
| u | objective function with penalty terms |
| \bar{x} | x -value of sample points |
| x | n -dimensional decision variable |
| y | objective value of f at x |

Greek symbols

| | |
|-----------------|-----------------------------------|
| α | regularization term of GPR |
| β | fluid bypass |
| γ | relaxation parameter |
| Δt | discrete time step, s |
| ϵ | effectiveness |
| λ, ρ | penalty weight vectors |
| μ | mean value |
| ξ | amount of exploration |
| Σ | covariance function |
| σ | standard deviation |
| Φ | cumulative distribution function |
| ϕ | probability distribution function |
| Ω | set of \mathbb{R}^n |

Subscripts and superscripts

| | |
|------|---------------------------------|
| 0 | starting condition |
| bc | best candidates |
| c | candidates |
| ch | charge mode |
| dch | discharge mode |
| f | thermal oil |
| grid | electricity grid |
| HTHP | high temperature heat pump |
| HTHX | high temperature heat exchanger |
| k | discrete time point |
| LTHX | low temperature heat exchanger |
| min | minimum value |
| p | pressure, N/m ² |
| s | storage |
| wt | wind turbine |

References

- [1] Xu Y., Yan C., Liu H., Wang J., Yang Z., Jiang Y., *Smart energy systems: A critical review on design and operation optimization*. Sustainable Cities and Society 2020;62, Article number:102369.
- [2] Lu Y., Wang S., Sun Y., Yan C., *Optimal scheduling of buildings with energy generation and thermal energy storage under dynamic electricity pricing using mixed-integer nonlinear programming*. Applied Energy 2015;147:49-58.
- [3] Sass S., Mitsos A., *Optimal operation of dynamic (energy) systems: When are quasi-steady models adequate?*. Computers and Chemical Engineering 2019;124:133-39.
- [4] Maleki A., Rosen M.A., Pourfayaz F., *Optimal Operation of a Grid-Connected Hybrid Renewable Energy System for Residential Applications*. Sustainability 2017;9:1-20.
- [5] Parisio A., Rikos E., Tzamalís G., Glielmo L., *Use of model predictive control for experimental microgrid optimization*. Applied Energy 2014;115:37-46.

- [6] Palma-Behnke R., Benavides C., Lanas F., Severino B., Reyes L., Llanos J., Sáez, D., *A Microgrid Energy Management System Based on the Rolling Horizon Strategy*. IEEE Transactions on Smart Grid 2013;4(2):996-1006.
- [7] Ma D., Zhang L., Sun B., *An interval scheduling method for the CCHP system containing renewable energy sources based on model predictive control*. Energy 2021;236, Article number:121418.
- [8] Nocedal J., Wright S. J., *Numerical Optimization*. New York, USA:Springer New York; 2006.
- [9] Hendrix E. M.T., Tóth B. G., *Introduction to Nonlinear and Global Optimization*. New York, USA:Springer New York; 2010.
- [10] Martí R., Lozano J. A., Mendiburu A., Hernando L., *Multi-start Methods*. In: Martí R., Pardalos P. M., Resende M. G. C., editors. Handbook of Heuristics. Springer, Cham. 2018. p. 155-75.
- [11] Pardalos P., Tawarmalani M., Sahinidis N. V., *Convexification and Global Optimization in Continuous and Mixed-Integer Nonlinear Programming*. Boston, MA: Springer US; 2002.
- [12] Parisio A., Rikos E., Glielmo L., *A Model Predictive Control Approach to Microgrid Operation Optimization*. IEEE Transactions on Control Systems Technology 2014;22(5):1813-27.
- [13] Bischi A., Taccari L., Martelli E., Amaldi E., Manzolini G., Silva P., Campanari S., Macchi E., *A detailed MILP optimization model for combined cooling, heat and power system operation planning*. Energy 2014;74:12-26.
- [14] Long Q., Wu C., *A Hybrid Method combining Genetic Algorithm and Hooke-Jeeves Method for constrained global optimization*. Journal of Industrial and Management Optimization 2014;10(4):1279–96.
- [15] Jeong S, Obayashi S., *Efficient Global Optimization (EGO) for Multi-Objective Problem and Data Mining*. IEEE Congress on Evolutionary Computation; 2005 Sep 02–05; Edinburgh, UK. IEEE:2138-45.
- [16] Lan G., Tomczak J. M., Roijers D. M., Eiben A.E., *Time efficiency in optimization with a bayesian-evolutionary algorithm*. Swarm and Evolutionary Computation 2022;69, Article number:100970.
- [17] Berk J., Nguyen V., Gupta S., Rana S., Venkatesh S., *Exploration Enhanced Expected Improvement for Bayesian Optimization*. In: Berlingerio M., Bonchi F., Gärtner T., Hurley N., Ifrim G., editors. European Conference: Machine Learning and Knowledge Discovery in Databases; 2018 Sep 10–14; Dublin, Ireland. Springer International Publishing:621-37.
- [18] Brochu E., Cora V. M., de Freitas N., *A tutorial on bayesian optimization of expensive cost functions, with application to active user modeling and hierarchical reinforcement learning*. ArXiv 2010;abs/1012.2599.
- [19] Hedar A. R., Fukushima M., *Hybrid Simulated Annealing and Direct Search Method for nonlinear unconstrained global optimization*. Optimization Methods and Software 2002;17(5):891-912.
- [20] Kelner V., Capitanescu F., Léonard O., Wehenkel L., *A hybrid optimization technique coupling an evolutionary and a local search algorithm*. Journal of Computational and Applied Mathematics 2008;215(2):448-56.
- [21] Cherki I., Chaker A., Djidar Z., Khalfallah N., Benzergua F., *A Sequential Hybridization of Genetic Algorithm and Particle Swarm Optimization for the Optimal Reactive Power Flow*. Sustainability 2019;11(14), Article number:3862.
- [22] Luo J., Chen Z., Zheng Y., *A gradient-based method assisted by surrogate model for robust optimization of turbomachinery blades*. Chinese Journal of Aeronautics 2022;35(10):1-7.
- [23] Zhang D., Zhang B., Wang Z., Zhu X., *An Efficient Surrogate-Based Optimization Method for BWBUG Based on Multifidelity Model and Geometric Constraint Gradients*. Mathematical Problems in Engineering 2021;2021:1-13.
- [24] Gao Y., Yu T., Li J., *Bayesian Optimization with Local Search*. In: Nicosia G., Ojha V., La Malfa E., Jansen G., Sciacca V., Pardalos P., Giuffrida G., Umeton R, editors. 6th International Conference: Machine Learning, Optimization, and Data Science; 2020 Jul 19–23; Siena, Italy. Springer International Publishing:350-61.
- [25] I. COIN-OR Foundation, *Interior point optimizer (ipopt)* Available at: <https://github.com/coin-or/Ipopt> [accessed 13.3.2023].

- [26] Wächter A., Biegler L. T., *On the implementation of an interior-point filter line-search algorithm for large-scale nonlinear programming*. Mathematical Programming 2006;106(1):25-57.
- [27] Rasmussen C. E., Williams C. K. I., *Gaussian Processes for Machine Learning*. The MIT Press; 2005.
- [28] Pedregosa F., Varoquaux G., Gramfort A., Michel V., Thirion B., Grisel O., Blondel M., Prettenhofer P., Weiss R., Dubourg V., Vanderplas J., Passos A., Cournapeau D., *Scikit-learn: Machine learning in Python*. Journal of machine learning research 2011;12(7):2825-30.
- [29] Hart W. E., Watson J. P., Woodruff D. L., *Pyomo: modeling and solving mathematical programs in Python*. Mathematical Programming Computation 2011;3(3):219-60.
- [30] Eriksson D., Poloczek M., *Scalable Constrained Bayesian Optimization*. In: Banerjee A., Fukumizu K, editors. Proceedings of The 24th International Conference on Artificial Intelligence and Statistics; 2021 Apr 13-15; San Diego, California, USA. PMLR:730-38.
- [31] Walden J. V. M., Bähr M., Glade A., Gollasch J., Tran A. P., Lorenz T., *Nonlinear operational optimization of an industrial power-to-heat system with a high temperature heat pump, a thermal energy storage and wind energy (accepted)*. Applied Energy (**online in 2023**).